Journal of Power Sources 196 (2011) 126–132

Contents lists available at ScienceDirect

Journal of Power Sources

journal homepage: www.elsevier.com/locate/jpowsour

Effect of sulfonated carbon nanofiber-supported Pt on performance of Nafion®-based self-humidifying composite membrane for proton exchange membrane fuel cell

T.F. Hung[a,b,*], S.H. Liao[a], C.Y. Li[a], Y.W. Chen-Yang[a,**]

[a] Department of Chemistry and Center for Nanotechnology, Chung Yuan Christian University, 200 Chung Pei Rd., Chung-Li, 32023, Taiwan, ROC
[b] Department of Chemistry, National Taiwan University, No. 1, Sec. 4, Roosevelt Road, Taipei, 10617, Taiwan, ROC

ARTICLE INFO

Article history:
Received 11 June 2010
Received in revised form 6 July 2010
Accepted 6 July 2010
Available online 13 July 2010

Keywords:
Sulfonation
Carbon nanofiber
Pt catalyst
Self-humidifying composite membrane
Proton exchange membrane fuel cell

ABSTRACT

In the present study, the Nafion®-based self-humidifying composite membrane (N-SHCM) with sulfonated carbon nanofiber-supported Pt (*s*-Pt/CNF) catalyst, N-*s*-Pt/CNF, is successfully prepared using the solution-casting method. The scanning electron microscopy-energy dispersive spectroscopy (SEM-EDS) images of N-*s*-Pt/CNF indicate that *s*-Pt/CNF is well dispersed in the Nafion® matrix due to the good compatibility between Nafion® and *s*-Pt/CNF. Compared with those of the non-sulfonated Pt/CNF-containing N-SHCM, N-Pt/CNF, the properties of N-*s*-Pt/CNF, including electronic resistivity, ion-exchange capacity (IEC), water uptake, dimensional stability, and catalytic activity, significantly increase. The maximum power density of the proton exchange membrane fuel cell (PEMFC) fabricated with N-*s*-Pt/CNF operated at 50 °C under dry H_2/O_2 condition is about 921 mW cm^{-2}, which is approximately 34% higher than that with N-Pt/CNF.

1. Introduction

Nafion® membrane, one of the perfluorosulfonic acid (PFSA) membranes, has been most widely used as the proton exchange membrane (PEM) for PEM fuel cell (PEMFC) due to its chemical stability, sufficient mechanical strength, and high proton conductivity under the hydrated state [1]. The proton conductivity of the Nafion® membrane depends significantly on its water content because the protons are transported through the hydrated ionic-clusters formed by the hydrophilic sulfonic groups attached to the polymer backbone [2,3]. Conventionally, the reactant gases have to be humidified prior to entering the PEMFC to maintain the satisfactory proton conductivity and to prevent the dehydration of the Nafion® membrane during operation. However, in this way, the external humidification units become a burden for the system, limiting the practical applications. Therefore, finding ways to avoid equipping the external humidification unit becomes an important challenge for PEMFC.

In response to this challenge, extensive efforts have been made by many research groups; the self-humidifying composite membranes (SHCMs) prepared by incorporating the platinum (Pt)-based catalysts into the membrane matrix have been progressively reported in recent years [1,4–19]. The results of these studies indicate that the performance efficiencies of the PEMFCs with the SHCMs are all better than those without the self-humidifying ability, particularly under dry fuel conditions. The result is principally ascribed to the presence of the Pt catalyst embedded in the SHCM, which is conceived to act as the water generation sites for the catalytic recombination of the fuels permeated through the membrane from the anode and the cathode.

On the other hand, the incorporation of the plain Pt nano-particles or the carbon-supported Pt (Pt/C) catalysts into the membrane may cause a short circuit of the SHCM because the electron-conducting paths may be formed by the networks of the plain Pt nano-particles or the Pt/C catalysts added [1,7,8]. To avoid the formation of the short circuit through the membrane, multi-layer configurations created by adding extra-plain Nafion® layers on one or two sides of the SHCM have been reported; the results show evident improvement on the issue of short circuit [1,7]. Nevertheless, the short circuit may be suppressed by the other methods, which can decrease the network of the filler added. Therefore, searching for methods to reduce the possibility of the network decreasing is also a crucial research topic.

Recently, the sulfonation of Pt/C catalyst has been investigated for the PEMFC electrode [20–22]. Easton et al. [20] and Xu et al. [21,22] chemically attached sulfonated silanes and sulfonic

* Corresponding author. Tel.: +886 2 3366 1169; fax: +886 2 2363 6359.
** Corresponding author. Tel.: +886 3 265 3317; fax: +886 3 265 3399.
E-mail addresses: taifeng@cycu.org.tw (T.F. Hung), yuiwhei@cycu.edu.tw (Y.W. Chen-Yang).

0378-7753/$ – see front matter.
doi:10.1016/j.jpowsour.2010.07.017

acid or short-chain sulfonic groups onto the surface of the carbon black-supported (Pt/CB) catalysts. Sulfonic groups grafted onto the surface of carbon nanotube-supported Pt (Pt/CNT) catalysts through the thermal decomposition of ammonium sulfate and *in situ* polymerization of 4-styrenesulfonate were also reported by Du et al. [23]. Evidently, using the resulting sulfonated Pt/C catalysts to prepare the gas diffusion electrodes (GDEs) not only showed much better cell efficiency than the un-sulfonated one, but also less Nafion® was required within the catalyst layers. This result can be ascribed to the sulfonated Pt/C catalysts that served as mixed electronic and protonic conductors, which significantly diminished the so-called triple-phase boundaries [20–22]. Although sulfonation of the Pt/C catalyst is a useful method to improve the Pt utilization by increasing the active triple-phase boundaries [23], most of the previous studies focused more on the electrode application.

In this study, a Nafion®-based self-humidifying composite membrane (N-SHCM) with sulfonated carbon nanofiber-supported Pt (*s*-Pt/CNF) catalyst, N-*s*-Pt/CNF, was prepared through a solution-casting method. As mentioned above, the hydrophilic sulfonic groups are attached to the polymer backbone of the Nafion® membrane. The compatibility between the Nafion® and the *s*-Pt/CNF was anticipated to improve significantly due to the presence of sulfonic groups grafted onto the Pt/CNF surface. Consequently, the *s*-Pt/CNF was well dispersed in the Nafion® matrix, resulting in the restraint of the formation of the *s*-Pt/CNF networks. The existence of the extra proton-conductive sulfonic groups was also beneficial because they provided more sites for the transportation of the protons. For these purposes, Pt/CNF synthesized from the microwave-assisted technology was sulfonated using the thermal process with the concentrated sulfuric acid. The resulting *s*-Pt/CNF was characterized by the wide-angle X-ray diffraction (WXRD) and the Fourier transform infrared (FT-IR) spectroscopy. The related properties of the as-prepared N-*s*-Pt/CNF, including electronic resistivity, ion-exchange capacity (IEC), water uptake, and dimensional stability, were discussed and compared with those of the Pt/CNF-containing N-SHCM (N-Pt/CNF) and a commercial Nafion® membrane (NRE 212). Moreover, the catalytic activities of the as-prepared N-SHCMs in the methanol electro-oxidation were determined using the cyclic voltammetric (CV) method. Finally, the effect of *s*-Pt/CNF on the performance of N-*s*-Pt/CNF for PEMFC was investigated under both humid and dry H_2/O_2 conditions.

2. Experimental details

2.1. Preparation of sulfonated carbon nanofiber-supported Pt (s-Pt/CNF) catalyst

To prepare the *s*-Pt/CNF, the Pt/CNF was firstly synthesized using microwave-assisted technology [24]. An ultrasonic processor with a frequency of 20 kHz (VCX 750, Sonics & Materials, Inc.) was used to disperse 0.04 g of carbon nanofibers (CNFs) (30–100 nm in diameter and 1–10 μm in length; Yonyu Applied Technology Material Co., Ltd., Taiwan) homogeneously in the Pt precursor solution consisting of 0.05 M hydrogen hexachloroplatinate(IV) hexahydrate (extra pure grade; Showa Chemicals Co., Ltd.), ethylene glycol (reagent grade; TEDIA Company Inc.), and 0.4 M potassium hydroxide (reagent grade; Shimakyu's Pure Chemicals).

The mixed solution was then placed in a domestic microwave oven (TMO-2030P, Taiwan, 2450 MHz, and 700 W) and heated for 90 s at 700 W. After being cooled to room temperature, the resulting suspension was filtered, and the residue was repeatedly washed with excess deionized water for at least five times. The as-synthesized Pt/CNF was finally dried with a freeze-dryer (Eyela FDU-1200, Tokyo Rikakikai) under 15 Pa at −50 °C. The amount of Pt deposited on the CNFs was 21 wt.%, which was determined by the thermogravimetric analysis (TGA) from room temperature to 900 °C with a heating rate of 10 °C min^{-1} under air flow of 60 mL min^{-1} [20]. Afterwards, the *s*-Pt/CNF was prepared by sulfonation of the Pt/CNF with the concentrated sulfuric acid (reagent grade; Showa chemicals Co., Ltd.) under nitrogen atmosphere at 160 °C for 24 h [25].

2.2. Preparation of Nafion®-based self-humidifying composite membrane (N-SHCM)

First, commercially available Nafion® membrane, NRE 212, which was purchased from DuPont Company, was purified according to well-known membrane cleaning procedures to remove the organic impurities prior to use [26]. The pretreated NRE 212 was immediately re-dissolved in the desired amount of *N*,*N*′-dimethylformamide (DMF; HPLC grade; TEDIA Company Inc.) to form a solution containing 5 wt.% of the Nafion®.

The Nafion®-based self-humidifying composite membrane (N-SHCM) with the *s*-Pt/CNF, N-*s*-Pt/CNF, was prepared using a solution-casting method. A designed amount of *s*-Pt/CNF was added into the 5 wt.% of Nafion®/DMF solution prepared above and dispersed by an ultrasonic processor to form a homogenous suspension. The resulting suspension was then cast into a stainless steel mold and evaporated slowly at 120 °C under vacuum to remove most of the solvent. The membrane was further heated to 160 °C and allowed to dry completely. The as-prepared N-*s*-Pt/CNF was cooled down to room temperature and purified again by the same procedures used for NRE 212 as described above. The thickness of N-*s*-Pt/CNF was 25 μm achieved by controlling the amount of Nafion®/DMF solution. The amount of Pt used in N-*s*-Pt/CNF was 0.02 mg cm^{-2}. For comparison, the Pt/CNF-containing N-SHCM, N-Pt/CNF, with the same Pt loading and thickness as in N-*s*-Pt/CNF was prepared also by the same procedures.

2.3. Characterizations and measurements

To identify the as-synthesized Pt catalysts, Pt/CNF and *s*-Pt/CNF, their wide-angle X-ray diffraction (WXRD) patterns were recorded from 20° to 100° at a scanning rate of 0.04° min^{-1} performed by the PANalytical PW3040/60X' Pert pro (45 kV, 40 mA) diffractometer with a copper target (λ = 1.541 Å). For each measurement, the sample was packed compactly and aligned perpendicularly to the diffraction axis. The average particle size for each as-synthesized Pt/CNF catalyst was estimated by calculating the width of the characteristic diffraction peak (1 1 1) according to the Debye–Scherrer formula (1) [27]:

$$d_{h,k,l} = \frac{0.89\lambda}{B_{h,k,l}\cos\theta} \quad (1)$$

where $d_{h,k,l}$ is the average particle size in nm, λ is the wavelength of the X-ray (1.541 Å), θ is the angle at the maximum of the peak, and $B_{h,k,l}$ is the measured peak width at half peak intensity.

Fourier transform infrared (FT-IR) spectra of the as-synthesized Pt/CNF catalysts were measured using a JASCO FT-IR-4200 spectrometer. Each specimen was prepared by making the KBr pellet composed of 100 mg of KBr (IR grade, ACROS Organic Company) and 2 mg of the Pt/CNF catalyst.

The surface morphologies of the N-SHCMs and their corresponding Pt mappings were investigated by the scanning electron microscope (SEM, Hitachi S-3500N) equipped with the energy-dispersive spectrometer (EDS, Noran Vantage DI instrument). Before measurement, each specimen was coated with a layer of carbon using a sputter coater to enhance the electrical conduction.

The electronic resistivity of each membrane was measured by a four-point probe method using the combined system of a current supplier (AUTOLAB PGST30, Eco Chemie) and a voltmeter (Keithley

196). The measured current density and voltage were then converted to the corresponding electronic resistivity (Ω cm) [28].

The ion-exchange capacity (IEC) of each membrane was determined by the typical titration method [29]. The dry membrane was soaked in a 1 M sodium chloride solution and carefully stirred with a magnetic stirrer for 12 h at the ambient temperature to ensure the protons were replaced completely by the sodium ions. This solution was subsequently titrated against a 0.01 M sodium hydroxide solution to neutralize the exchanged protons using the phenolphthalein (Indicator grade, ACROS Organic Company) as an indicator. After that, the calculated IEC value was obtained through Eq. (2):

$$\mathrm{IEC} = \frac{V \times M}{m} \tag{2}$$

where IEC is the ion-exchange capacity (mequiv. g^{-1}); V is the added titrant volume at the equivalent point (mL); M is the molar concentration of the titrant; m is the dry membrane weight (g).

Water uptake of each membrane was calculated from Eq. (3), W_1 is the net weight of the dry membrane after drying at 80 °C in the vacuum oven for 24 h and W_2 is the weight of the wet membrane soaked in the deionized water at 80 °C for 24 h:

$$\Delta W(\mathrm{wt.\%}) = \frac{W_2 - W_1}{W_1} \times 100\% \tag{3}$$

For measuring the dimensional stability of each membrane, the specimen with the area of 6 cm × 5 cm was stored at the vacuum oven of 80 °C for 24 h. Areal change (ΔA) was calculated by measuring the area of the specimen before (A_1) and after (A_2) soaking in the deionized water at 80 °C for 24 h, as expressed in Eq. (4):

$$\Delta A(\%) = \frac{A_2 - A_1}{A_1} \times 100\% \tag{4}$$

All the results, including the electronic resistivity, IEC, water uptake and dimensional stability, were determined with the standard deviations based on the measurements of three samples for each Pt/CNF catalyst and membrane.

The catalytic activity of each N-SHCM in the methanol electrooxidation was determined by the cyclic voltammetric (CV) method. The electrolyte used in this measurement was composed of 1 M methanol and 1 M sulfuric acid solution. The N-SHCM was used as the working electrode. The Ag/AgCl electrode (Model 6.0733.100, Metrohm, Switzerland, 0.207 V at 25 °C) and the platinum electrode (Model 6.0301.100, Metrohm, Switzerland) were used as the reference and the counter electrode, respectively. The measurements were performed in the conventional three-electrode test cell which was connected with the electrochemical analyzer (AUTOLAB PGST30, Eco Chemie) under the sweep rate of 5 mV s^{-1} from −0.1 to 0.9 V at room temperature. During the test, a high-purity Nitrogen gas was carefully purged in the electrolyte to minimize the oxygen contamination.

2.4. Fabrication of membrane electrode assembly (MEA) and cell efficiency test

The MEAs with an active area of 5 cm^2 were fabricated by the hot-pressing procedure at 130 °C under 30 kg cm^{-2} for 5 min. The woven web-based gas diffusion electrodes (GDEs), LT 140E-W, were purchased from BASF Fuel Cell, Inc., USA. The amount of Pt used for the anode and cathode was 0.5 mg cm^{-2}. To minimize the interfacial resistance between the N-SHCM and GDEs, the 5 wt.% of Nafion® solution diluted from a commercially available 20 wt.% of Nafion® solution (DE 2020, DuPont) was coated on the electrode surface using the brush method. The solid content of the loaded Nafion® was restricted to 1.8 mg cm^{-2} for each electrode.

The corresponding single-cell fixture was composed of the as-prepared MEA and a pair of graphite plates with a serpentine flow channel of 1 mm width and 1 mm depth. To circumvent the GDE getting into the channels, the MEA (0.5 ± 0.02 mm in thickness) was placed between a pair of PTFE gaskets, each of which has a thickness of 0.25 mm. Next, the MEA was clamped between two stainless end plates, with eight bolts tightened to a uniform torque of 2.94 N m in order to ensure that the MEA comes into close contact with the graphite plates without getting into the channels.

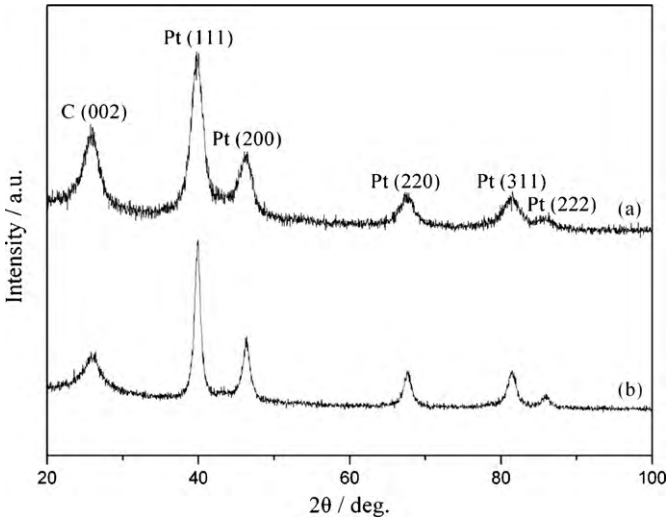

Fig. 1. XRD patterns of (a) Pt/CNF and (b) *s*-Pt/CNF.

During the test operation, the single-cell fixture was connected to an in-house fuel cell test station composed of an electronic load (Chroma 63030, Chroma Ate Inc.), potentiostat/galvanostat instrument (AUTOLAB PGST30, Eco Chemie) and a bubble-type humidifier. The fuel of the anode was hydrogen, and that of the cathode was oxygen. Before the cell test, a leak test was performed using nitrogen gas to ensure that the single cell was gastight. Afterwards, a constant current mode was applied to activate the MEA. In the measurement, the electronic load was controlled by the software Nova version 1.3 and interfaced by a computer for data collection. The cell test was carried out under humidified and dry H_2/O_2 conditions, respectively. For both conditions, the flow rate of the anode and cathode was 70 and 102 mL min^{-1}, respectively (corresponding to 1.6/2.3 of the stoichiometric ratio). For the humidified H_2/O_2 condition, the operating temperatures of the anode humidifier, the cathode humidifier, and the cell were all set to 50 °C, while the cell was operated at 50 °C in dry H_2/O_2 condition. The test was operated under an atmospheric pressure, and the cell performances were obtained by controlling the cell current and recording the corresponding stabilized voltage.

3. Results and discussion

3.1. Characterizations of s-Pt/CNF

The as-synthesized Pt/CNF catalysts, non-sulfonated and sulfonated by thermal process with concentrated sulfuric acid, were analyzed by XRD and their corresponding patterns are shown in Fig. 1. The characteristic diffraction peaks of Pt crystal for the non-sulfonated Pt/CNF catalyst (Fig. 1(a)) are clearly seen at the Bragg angles of 40°, 46°, 68°, 81°, and 83°. These peaks correspond to the results reported in [23,30,31] and can be indexed to the (1 1 1), (2 0 0), (2 2 0), (3 1 1), and (2 2 2) planes of the face-centered cubic (fcc) Pt, respectively. This result indicates that the Pt/CNF was successfully synthesized using the microwave-technique for 90 s. The XRD pattern recorded for the sulfonated Pt/CNF, *s*-Pt/CNF is presented in Fig. 1(b). It exhibits a similar characteristic diffraction

Table 1
Measurement parameters of the XRD.

	s-Pt/CNF	Pt/CNF
h k l	1 1 1	1 1 1
λ (Å)	1.541	1.541
B_{111} (°)	0.996	1.847
Bragg, 2θ (°)	39.877	39.814
Pt size (nm)	8.39	4.53

pattern as the Pt/CNF in terms of peak position and intensity. However, the *s*-Pt/CNF obviously shows sharper XRD peaks than those of the non-sulfonated Pt/CNF, indicating that the *s*-Pt/CNF presents a larger particle size than that of the non-sulfonated one. The main XRD parameters of the Pt X-ray diffraction and calculation results are listed in Table 1. The average Pt particle size for the Pt/CNF and *s*-Pt/CNF are calculated to be 4.53 nm and 8.39 nm, respectively, from the (1 1 1) diffraction peaks using the Debye–Scherrer formula [27]. The significant increase in Pt particle size is probably due to the facile agglomeration of nano-scale Pt particles on the CNF surface at high thermal-treating temperature [23].

Fig. 2 shows the FT-IR spectra of Pt/CNF and *s*-Pt/CNF. Compared with the spectrum of Pt/CNF (Fig. 2(a)), the new absorption peaks observed at 1065 and 1174 cm^{-1} of *s*-Pt/CNF in Fig. 2(b) are assigned to the symmetric and asymmetric stretching vibrations of the sulfonic group, respectively. This finding confirms that the sulfonic groups were successfully grafted onto the *s*-Pt/CNF surface.

3.2. Sulfonation effect of Pt/CNF on the compatibility and properties of N-SHCM

To investigate the sulfonation effect of Pt/CNF on the compatibility of *s*-Pt/CNF with the Nafion® matrix and the properties of the Nafion®-based self-humidifying composite membrane (N-SHCM), the as-prepared Pt/CNF before and after sulfonation was

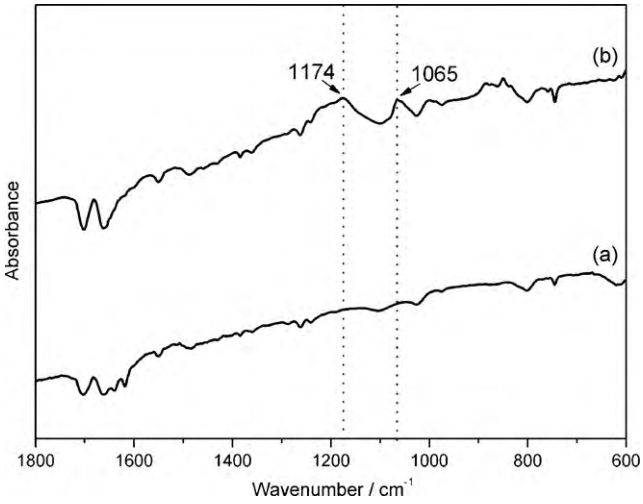

Fig. 2. FT-IR spectra of (a) Pt/CNF and (b) *s*-Pt/CNF.

used to prepare the N-SHCMs, respectively. The scanning electron microscopy (SEM) micrographs and their corresponding energy dispersive spectroscopy (EDS) Pt mappings for the surface of the N-SHCMs, N-Pt/CNF, and N-*s*-Pt/CNF are presented in Fig. 3. Compared with the SEM morphology of N-Pt/CNF shown in Fig. 3(a), a smooth surface is exhibited for N-*s*-Pt/CNF in Fig. 3(b), implying that no agglomeration was observed in N-*s*-Pt/CNF and that *s*-Pt/CNF was better dispersed in the Nafion® matrix than Pt/CNF. This is further confirmed by the corresponding EDS Pt mappings shown in Fig. 3(d). The tremendous improvement in the dispersion of *s*-Pt/CNF in the Nafion® matrix is attributed to the better compatibility between the Nafion® and *s*-Pt/CNF due to the presence of the grafted sulfonic groups in *s*-Pt/CNF.

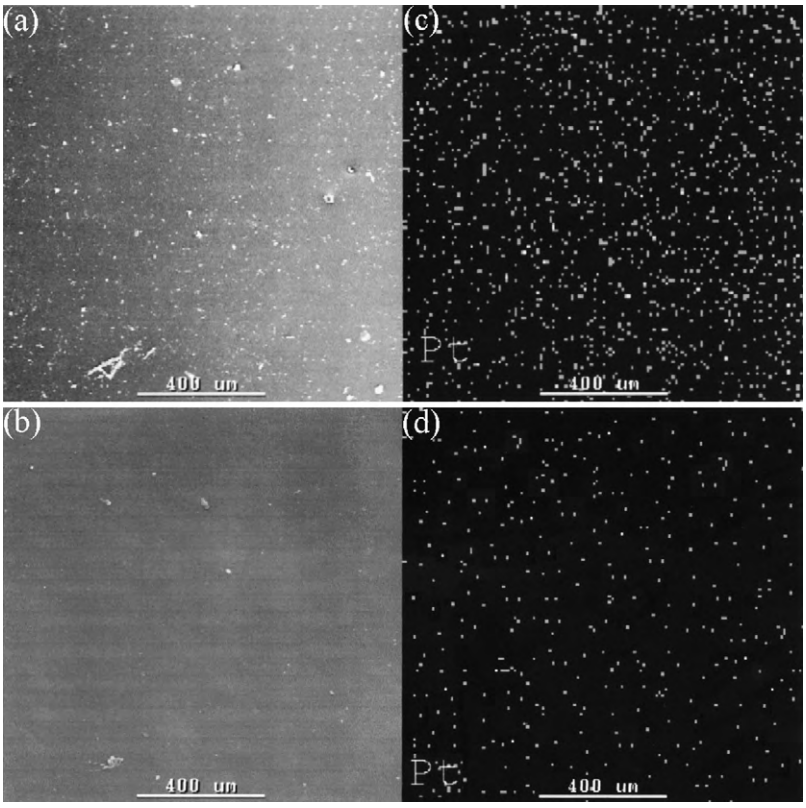

Fig. 3. SEM microphotographs (left) and the corresponding EDS Pt mappings (right) of the top-view of (a) N-Pt/CNF and (b) N-*s*-Pt/CNF.

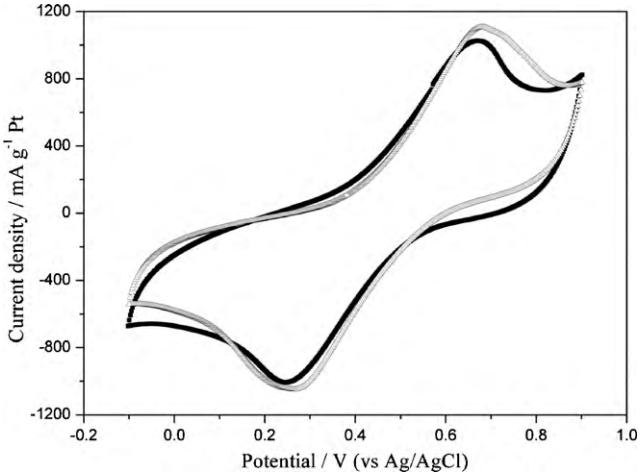

Fig. 4. Cyclic voltammograms of (■) N-Pt/CNF and (△) N-*s*-Pt/CNF.

Table 2 lists the values of the electronic resistivity, ion-exchange capacity (IEC), water uptake, and areal change for the N-SHCMs and the NRE 212. As indicated, the electronic resistivity of N-Pt/CNF evidently decreased with the addition of Pt/CNF into the Nafion® matrix. Nevertheless, the electronic resistivity of N-*s*-Pt/CNF was about 40-fold higher than that of N-Pt/CNF, implying that the electrons were much more difficult to transport in N-*s*-Pt/CNF than N-Pt/CNF. This can be ascribed to the fact that *s*-Pt/CNF was much better separated in the Nafion® matrix than the Pt/CNF due to the better compatibility as discussed above, resulting in a smaller network formed by *s*-Pt/CNF and a decreased electron-conduction in N-*s*-Pt/CNF.

As indicated in Table 2, the order of the IEC values for these membranes is N-*s*-Pt/CNF > NRE 212 > N-Pt/CNF. This order implies that more sulfonic groups were in N-*s*-Pt/CNF than NRE 212, and it is ascribed to the presence of the sulfonic groups in the *s*-Pt/CNF that are beneficial to the increase in water uptake and proton-conducting abilities. In fact, a similar trend is obtained in the water uptake as indicated in the table; approximately 29% more water was uptaken by N-*s*-Pt/CNF than by NRE 212. By increasing the water absorbed, the dimensional stability of the membrane was supposed to decrease significantly because the swelling ability of the membrane was considered to increase. However, the areal changes of both N-Pt/CNF and N-*s*-Pt/CNF listed in Table 2 were approximately 73% and 41% lower than that of NRE 212, respectively. This is attributed to the intrinsic mechanical property of CNF and the good compatibility between the *s*-Pt/CNF and Nafion® matrix, which results in restraining the swelling of the membrane effectively [7]. Further, the more areal change for N-*s*-Pt/CNF than for N-Pt/CNF is attributed to its higher water uptake ability.

3.3. Catalytic activity of N-SHCMs

Fig. 4 shows the cyclic voltammograms of the as-prepared N-SHCMs measured in the CH_3OH/H_2SO_4 solution from −0.1 to 0.9 V with 5 mV s^{-1} of the sweep rate. The oxidative peaks of the methanol occurred at 0.67 and 0.68 V for N-Pt/CNF and N-*s*-Pt/CNF, respectively, which are in the range of 0.67–0.72 V reported for the typical Pt/C catalysts [32,33]. The current density of the oxidative peak, I_{ap}, for N-*s*-Pt/CNF is 1108 mA g^{-1}, which is approximately 8% higher than that for N-Pt/CNF. Although the average Pt particle size for the *s*-Pt/CNF calculated using the Debye–Scherrer formula is larger than that for the non-sulfonated Pt/CNF, less agglomerations of the *s*-Pt/CNF were observed in N-*s*-Pt/CNF as evidenced in Fig. 3(d). The slight increase in the current density for N-*s*-Pt/CNF can be ascribed to the better dispersion of *s*-Pt/CNF than of Pt/CNF in the Nafion® matrix as discussed above. This shows that the increased Pt particle size for the *s*-Pt/CNF does not significantly affect the catalytic activity of N-*s*-Pt/CNF. The result suggests that the as-prepared N-*s*-Pt/CNF has better catalytic activity to carry out the recombination reaction of the fuels for generating water to assist the proton transport.

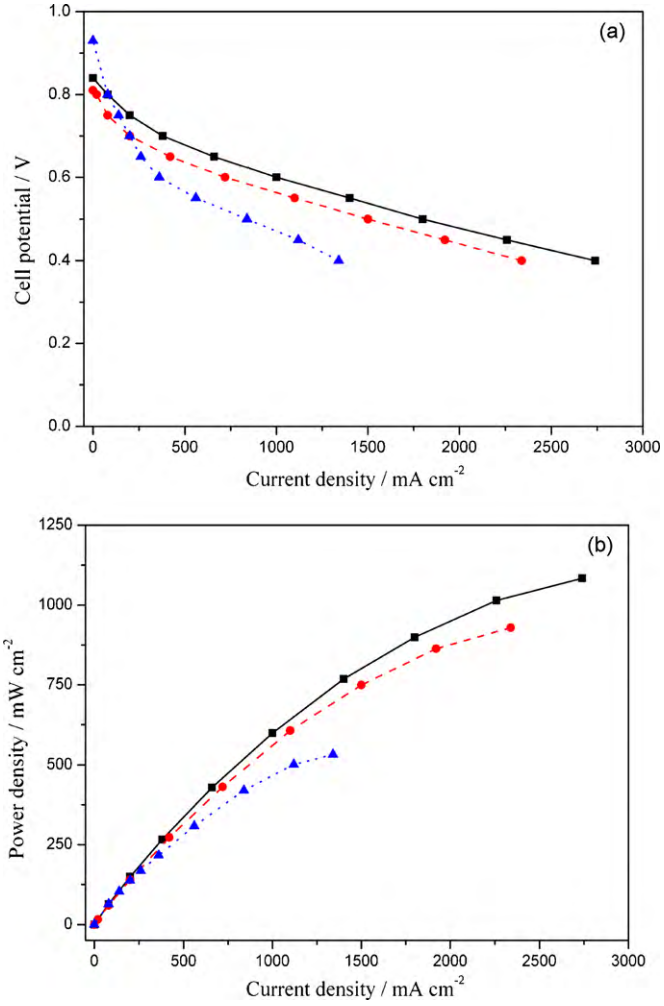

Fig. 5. Polarization curves of PEMFC measured in the humidified H_2/O_2 system (a) *I–V* and (b) *I–P* curves (■) FC-1, (●) FC-2, and (▲) FC-3.

3.4. Cell performance of PEMFC test

To study the sulfonation effect of Pt/CNF on the performance of the corresponding PEMFC, the MEAs for the preparation of the PEMFCs, FC-1, FC-2, and FC-3 were fabricated with N-*s*-Pt/CNF, N-Pt/CNF, and NRE 212, respectively. Fig. 5 plots the polarization curves of the as-prepared PEMFCs measured under the humidified H_2/O_2 condition. As depicted in Fig. 5(a), a higher open circuit potential (OCP) of FC-3 is exhibited, which is more likely due to the higher electronic resistivity and lower hydrogen crossover of NRE 212 [7]. Nevertheless, a decrease in *I–V* performance of the FC-3 was clearly observed in the range of 0.8–0.5 V. This finding implies that the potential drops of FC-1 and FC-2 caused by ohmic overpotentials were less than those of FC-3, that is, there was less resistance loss for FC-1 and FC-2 than for FC-3. This can be attributed to the self-humidifying ability of the N-SHCM, resulting in the improvement of cell efficiency. The best current and power densities of FC-1 at 0.4 V were 2740 mA cm^{-2} and 1084 mW cm^{-2},

Table 2
Comparison of the electrical and physical properties between N-SHCMs and NRE 212.

Membrane designation	Electronic resistivity (Ω cm)	Ion-exchange capacity, IEC (mequiv. g^{-1})	Water uptake (wt.%)	Areal change (%)
N-*s*-Pt/CNF	610 ± 8	1.12 ± 0.02	36 ± 2	13 ± 1
N-Pt/CNF	15 ± 2	0.90 ± 0.01	25 ± 1	6 ± 1
NRE 212	12096 ± 15	0.93 ± 0.02	28 ± 1	22 ± 2

Table 3
Comparison of the fraction of current densities delivered by a PEMFC fabricated with the N-*s*-Pt/CNF, N-Pt/CNF and NRE 212 membranes operating under dry H_2 and O_2.

Membrane designation	Fraction of current density at the voltage of different voltage[a] (%)				
	0.8 V	0.7 V	0.6 V	0.5 V	0.4 V
N-*s*-Pt/CNF	50.0	42.1	40.0	76.7	84.7
N-Pt/CNF	–	20.0	36.1	65.3	74.4
NRE 212	–	–	–	0.5	0.7

[a] The fraction of current density was calculated in comparison to that obtained on operating with humidified H_2 and O_2.

respectively. These values are approximately 105% higher than the values obtained from FC-3 (i.e., 1340 mA cm^{-2} and 533 mW cm^{-2}).

On the other hand, under the dry H_2/O_2 condition, the dramatic decreases in the OCP and cell efficiency are clearly observed for FC-3 in Fig. 6. The power density of FC-3 output at 0.4 V was only 3.8 mW cm^{-2} because the NRE 212 membrane was not hydrated under the dry condition, resulting in the difficulty in proton transport. The result confirms that the Nafion® membrane is not suitable to operate under dry conditions as expected. However, both the OCP values and the performances of the PEMFCs fabricated with the as-prepared N-SHCMs significantly improved under the dry condition. The current and power densities obtained from FC-2 were 1740 mA cm^{-2} and 688 mW cm^{-2}, respectively, indicating that the Pt present in the N-SHCM plays a critical role in the catalytic recombination of the reactant fuels permeating through the membrane. With the same Pt loading, the power density of FC-1 was further increased to 921 mW cm^{-2}, which was about 34% higher than that of FC-2. Based on the same thickness of N-SHCMs, the significant enhancement is ascribed to the higher catalytic activity of N-*s*-Pt/CNF, which generates water more efficiently. In addition, the higher IEC value contributed by the extra sulfonic groups grafted onto the *s*-Pt/CNF is also beneficial to increase the proton transport.

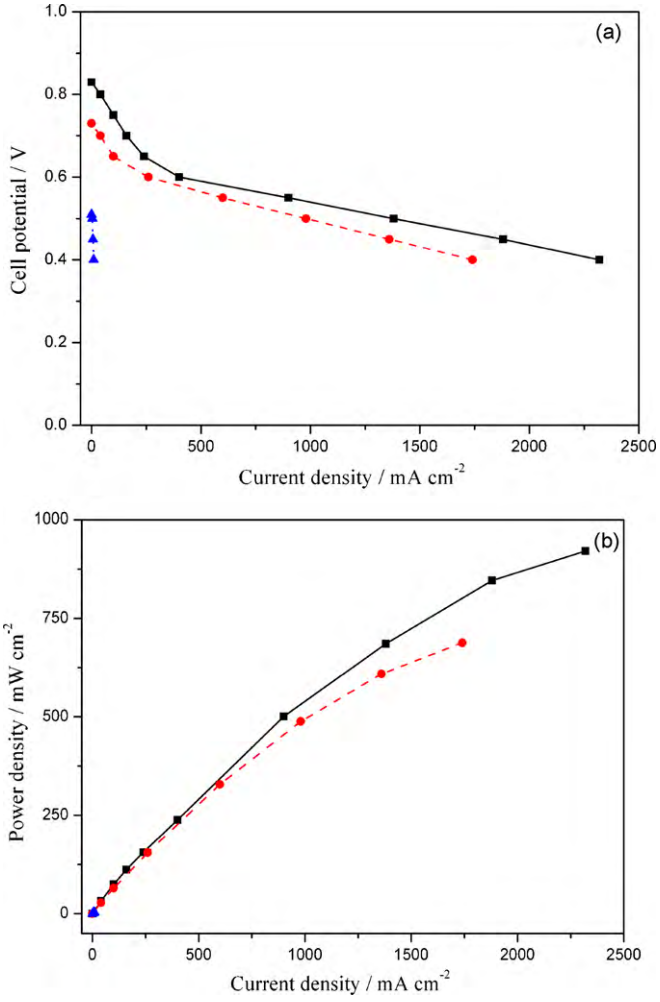

Fig. 6. Polarization curves of PEMFC measured in the dry H_2/O_2 system (a) *I–V* and (b) *I–P* curves (■) FC-1, (●) FC-2, and (▲) FC-3.

The relative currents generated at different cell voltages with the dry H_2 and O_2 compared with those obtained with humidified reactants for the MEAs fabricated with N-*s*-Pt/CNF, N-Pt/CNF, and NRE 212 membranes are shown in Table 3. The fraction of current density was calculated in comparison with that obtained from operating with humidified H_2 and O_2. The fractions of current density delivered with the N-*s*-Pt/CNF membrane are higher than those delivered with the N-Pt/CNF and NRE 212 membranes. For example, the cell with the N-Pt/CNF membrane with dry reactants generates 20–74% of the current generated with humidified reactants at a cell voltage of 0.7–0.4 V. On the other hand, the cell with N-*s*-Pt/CNF membrane generates 42–85% of the current under similar conditions. These results indicate the pronounced effect of the incorporated *s*-Pt/CNF catalyst in self-humidifying composite membrane and the improvement of cell performance with dry reactants.

4. Conclusions

Nafion®-based self-humidifying composite membrane (N-SHCM) with the sulfonated carbon nanofiber-supported Pt (*s*-Pt/CNF) catalyst, N-*s*-Pt/CNF, was successfully prepared in the present study through a solution-casting method. The XRD result showed that the Pt/CNF was successfully synthesized using the microwave-technique, whereas FT-IR spectrum indicated that the sulfonic groups were successfully grafted on the *s*-Pt/CNF by thermal reaction of the Pt/CNF with the concentrated sulfuric acid. The images of SEM-EDS show that *s*-Pt/CNF was better dispersed in the Nafion® matrix, confirming that the compatibility between Nafion® and *s*-Pt/CNF was significantly improved due to the sulfonation. Comparing with that of non-sulfonated Pt/CNF-containing N-SHCM, N-Pt/CNF, the electronic resistivity of N-*s*-Pt/CNF was about 40-fold higher. Moreover, the related properties of N-*s*-Pt/CNF, including ion-exchange capacity (IEC), water uptake, dimensional stability, and catalytic activity, significantly increased due to the

presence of the sulfonic groups grafted onto the *s*-Pt/CNF surface. Furthermore, the performance of the PEMFC with N-*s*-Pt/CNF operated at 50 °C under dry H_2/O_2 condition was about 34% higher than that with N-Pt/CNF. The results suggest that the as-prepared N-*s*-Pt/CNF is a good candidate for the preparation of N-SHCM, which can be applied in PEMFC to be used under dry conditions.

Acknowledgements

This research was financially supported by National Science Council, ROC (99-2623-E-033-001-ET), and the projects of the specific research fields in Chung Yuan Christian University, Taiwan, under grant number CYCU-98-CR-CH. We greatly appreciate the assistance given by the Precision Instrument Center at the National Central University in the SEM-EDS analysis.

References

[1] B. Yang, Y.Z. Fu, A. Manthiram, J. Power Sources 139 (2005) 170–175.
[2] T.A. Zawodzinski, C. Derouin, S. Radzinski, R.J. Sherman, V.T. Smith, T.E. Springer, S. Gottesfeld, J. Electrochem. Soc. 140 (1993) 1041–1047.
[3] Y. Sone, P. Ekdunge, D. Simonsson, J. Electrochem. Soc. 143 (1996) 1254–1259.
[4] T. Yang, Int. J. Hydrogen Energy 33 (2008) 2530–2535.
[5] H.K. Lee, J.I. Kim, J.H. Park, T.H. Lee, Electrochim. Acta 50 (2004) 761–768.
[6] C. Wang, Z.X. Liu, Z.Q. Mao, J.M. Xu, K.Y. Ge, Chem. Eng. J. 112 (2005) 87–91.
[7] Y.H. Liu, B.L. Yi, Z.G. Shao, L. Wang, D.M. Xing, H.M. Zhang, J. Power Sources 163 (2007) 807–813.
[8] D.H. Son, R.K. Sharma, Y.G. Shul, H.S. Kim, J. Power Sources 165 (2007) 733–738.
[9] W.J. Zhang, M.K. Li, P.L. Yue, P. Gao, Langmuir 24 (2008) 2663–2670.
[10] F.Q. Liu, B.L. Yi, D.M. Xing, J.R. Yu, Z.J. Hou, Y.Z. Fu, J. Power Sources 124 (2003) 81–89.
[11] S.C. Mu, X. Wang, H.L. Tang, P.G. Li, M. Lei, M. Pan, R.Z. Yuan, J. Electrochem. Soc. 153 (2006) A1868–A1872.
[12] X.B. Zhu, H.M. Zhang, Y.M. Liang, Y. Zhang, B.L. Yi, Electrochem. Solid State Lett. 9 (2006) A49–A52.
[13] X.B. Zhu, H.M. Zhang, Y. Zhang, Y.M. Liang, X.L. Wang, B.L. Yi, J. Phys. Chem. B 110 (2006) 14240–14248.
[14] L. Wang, D.M. Xing, Y.H. Liu, Y.H. Cai, Z.G. Shao, Y.F. Zhai, H.X. Zhong, B.L. Yi, H.M. Zhang, J. Power Sources 161 (2006) 61–67.
[15] Y. Zhang, H.M. Zhang, Y.F. Zhai, X.B. Zhu, C. Bi, J. Power Sources 168 (2007) 323–329.
[16] Y. Zhang, H.M. Zhang, C. Bi, X.B. Zhu, Electrochim. Acta 53 (2008) 4096–4103.
[17] D.M. Xing, B.L. Yi, Y.Z. Fu, F.Q. Liu, H.M. Zhang, Electrochem. Solid State Lett. 7 (2004) A315–A317.
[18] Y. Zhang, H.M. Zhang, X.B. Zhu, L. Gang, C. Bi, Y.M. Liang, J. Power Sources 165 (2007) 786–792.
[19] L. Wang, B.L. Yi, H.M. Zhang, D.M. Xing, Polym. Adv. Technol. 19 (2008) 1809–1815.
[20] E.B. Easton, Z.G. Qi, A. Kaufman, P.G. Pickup, Electrochem. Solid State Lett. 4 (2001) A59–A61.
[21] Z. Xu, Z. Qi, A. Kaufman, Electrochem. Solid State Lett. 6 (2003) A171–A173.
[22] Z.Q. Xu, Z.G. Qi, A. Kaufman, Electrochem. Solid State Lett. 8 (2005) A313–A315.
[23] C.Y. Du, T.S. Zhao, Z.X. Liang, J. Power Sources 176 (2008) 9–15.
[24] H.W. Wang, R.X. Dong, H.Y. Chang, C.L. Liu, Y.W. Chen-Yang, Mater. Lett. 61 (2007) 830–833.
[25] X.H. Mo, D.E. López, K. Suwannakarn, Y.J. Liu, E. Lotero, J.G. Goodwin Jr., C.Q. Lu, J. Catal. 254 (2008) 332–338.
[26] J. Moreira, A.L. Ocampo, P.J. Sebastian, M.A. Smit, M.D. Salazar, P. del Angel, J.A. Montoya, R. Pérez, L. Martínez, Int. J. Hydrogen Energy 28 (2003) 625–627.
[27] V. Radmilovic, H.A. Gasteiger, J.P. Ross, C.S. Lecea, J. Catal. 154 (1995) 98–106.
[28] S.M. Sze, Physics of Semiconductor Device, 2nd ed., John-Wiley & Sons, New York, 1981, pp. 30–32.
[29] K.T. Park, U.H. Jung, D.W. Choi, K. Chun, H.M. Lee, S.H. Kim, J. Power Sources 177 (2008) 247–253.
[30] J.B. Joo, P. Kim, W. Kim, J. Kim, J. Yi, Catal. Today 111 (2006) 171–175.
[31] W. Li, C. Liang, W. Zhou, J. Qiu, Z. Zhou, G. Sun, Q. Xin, J. Phys. Chem. B 107 (2003) 6292–6299.
[32] M.H. Seo, S.M. Choi, H.J. Kim, J.H. Kim, B.K. Cho, W.B. Kim, J. Power Sources 179 (2008) 81–86.
[33] H.J. Wang, H. Yu, F. Peng, P. Lv, Electrochem. Commun. 8 (2006) 499–504.